ACS Catalysis

Letter

pubs.acs.org/acscatalysis

Huge Instability of Pt/C Catalysts in Alkaline Medium

Anicet Zadick,*[,¶,†,‡] Laetitia Dubau,[¶,†,‡] Nicolas Sergent,[†,‡] Grégory Berthomé,[§,∥] and Marian Chatenet*[,¶,†,‡,⊥]

[†]University Grenoble Alpes, LEPMI, F-38000 Grenoble, France

[‡]CNRS, LEPMI, F-38000 Grenoble, France

[§]University Grenoble Alpes, SIMAP, F-38000 Grenoble, France

[∥]CNRS, SIMAP, F-38000 Grenoble, France

[⊥]French University Institute (IUF), Paris, France

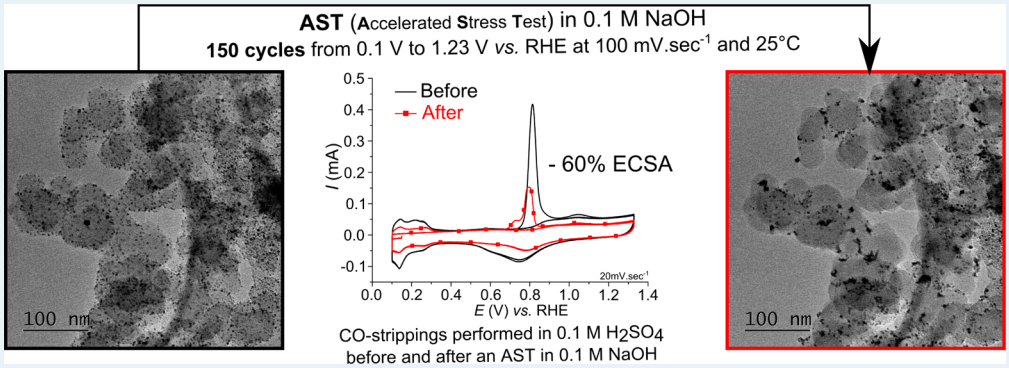

ABSTRACT: The stability of carbon-supported electrocatalysts has been largely investigated in acidic electrolytes, but the literature is much scarcer regarding similar stability studies in alkaline medium. Herein, the degradation of Vulcan XC-72-supported platinum nanoparticles (noted Pt/C), a state-of-the-art proton exchange membrane fuel cell electrocatalyst, is investigated in alkaline medium by combining electrochemical measurements and identical location transmission electron microscopy; electrochemical surface area (ECSA) losses were bridged to electrocatalyst morphological changes. The results demonstrate that the degradation in 0.1 M NaOH at 25 °C is severe (60% of ECSA loss after only 150 cycles between 0.1 and 1.23 V vs RHE), which is about 3 times worse than in acidic media for this soft accelerated stress test. Severe carbon corrosion has been ruled out according to Raman spectroscopy and X-ray photoelectron spectroscopy measurements, and it seems that the chemistry of the carbon support (in particular, the interface (chemical bounding)) between the Pt nanoparticles and their carbon substrate does play a significant role in the observed degradations.

KEYWORDS: *alkaline electrolytes, carbon-supported platinum nanoparticles (Pt/C), high-surface-area carbon, durability, identical location transmission electron microscopy (ILTEM), Raman spectroscopy*

1. INTRODUCTION

Platinum (and platinum alloy) nanoparticles supported on high-surface-area carbon, an inexpensive, easily structured, and conductive material, are the state-of-the-art electrocatalyst for fuel cell applications.[1,2] It is no secret that these materials undergo severe degradation at the cathode of proton exchange membrane fuel cells;[3−5] as such Pt/C degradations that have been massively investigated at high potential values (above 0.6 V vs RHE) and in acidic media, especially for the oxygen reduction reaction (ORR).[6−9] In contrast, almost no studies have been conducted for an application as an electrode material in (direct) alkaline fuel cells (i.e., in alkaline media), except investigations at bulk platinum (and bulk gold) surfaces.[10] Herein, the stability of a state-of-the-art Pt/C electrocatalyst is compared in alkaline and acidic media by correlating the results of electrochemical characterizations, identical location transmission electron microscopy (ILTEM) imaging, and physicochemical analyses (Raman spectroscopy and X-ray photoelectron spectroscopy, XPS).

2. EXPERIMENTAL SECTION

The Pt/C catalyst was purchased from E-Tek (20% weight fraction, Vulcan XC72 carbon black substrate) and used as-received without any further treatment. A catalyst ink was prepared by mixing 10 mg of catalyst powder, 7.74 mL of MQ-grade water (18.2 MΩ cm, <3 ppb total organic carbon, Elix + Milli-Q Gradient, Millipore), 18.3 μL of 5 wt % Nafion solution (Electrochem. Inc.), and 33.9 μL of isopropyl alcohol. After 30 min of ultrasonic stirring before each experiment, 10 μL of this ink was deposited on a 5 mm-diameter glassy-carbon electrode

Received: May 19, 2015
Revised: July 10, 2015
Published: July 15, 2015

DOI: 10.1021/acscatal.5b01037
ACS Catal. 2015, 5, 4819−4824

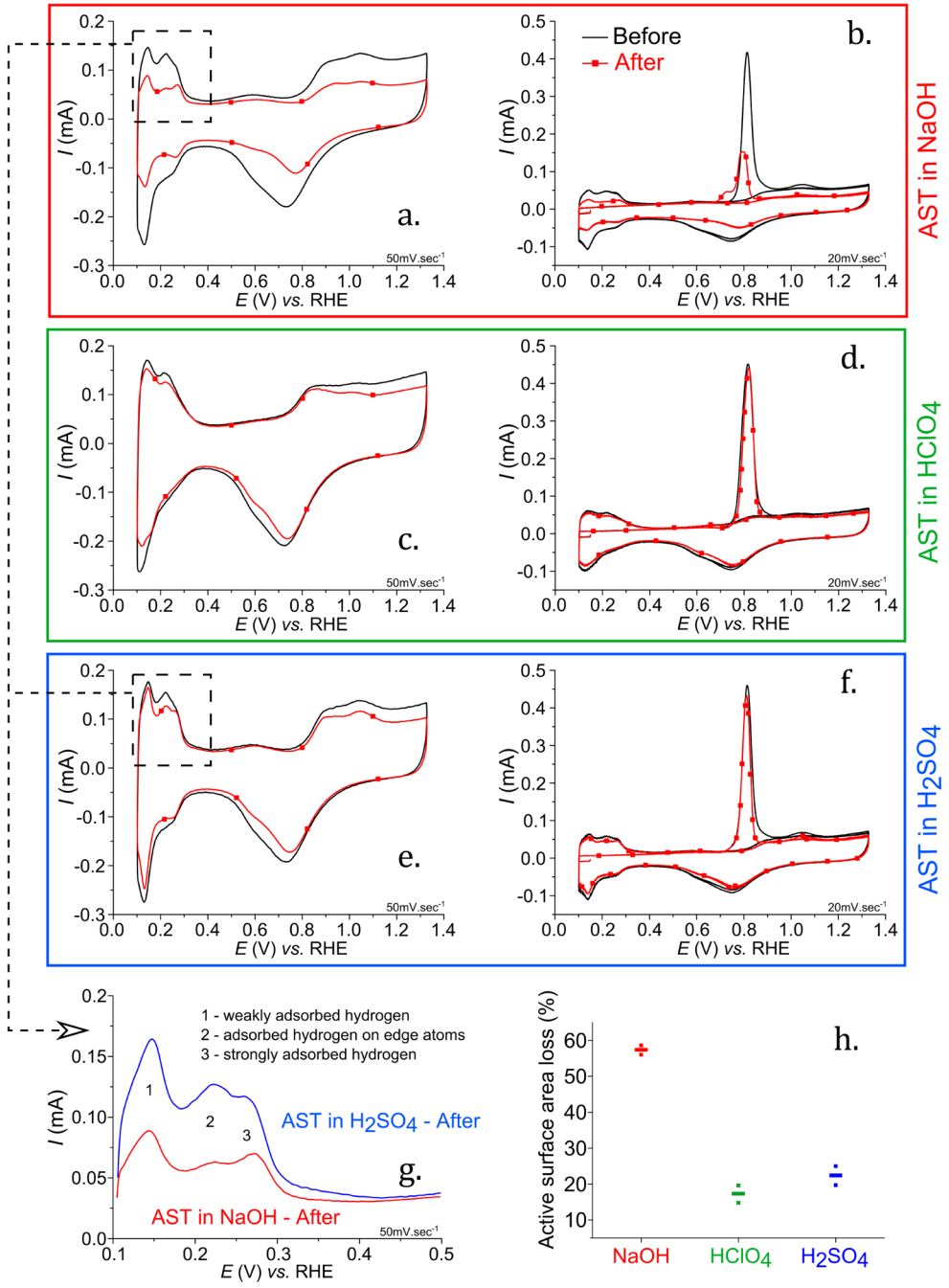

Figure 1. Characterization and CO-stripping voltammograms carried out in 0.1 M H_2SO_4 solution at 25 °C before and after AST performed in (a, b) NaOH, (c, d) $HClO_4$, or (e, f) H_2SO_4. (g) Comparison of characterization voltammograms performed after an AST in NaOH and in H_2SO_4 solutions. (h) Corresponding relative active surface-area losses for each electrolyte medium.

(13.07 μg_{Pt} cm^{-2} over the electrode surface), previously polished until 1 μm with diamond paste and copiously rinsed in acetone, ethanol, and water, successively.

The accelerated stress tests (AST) were performed in a 0.1 M solution of H_2SO_4, $HClO_4$, and NaOH; the high-purity reagents were all provided by Merck (Suprapur quality), and the electrolytic solutions were prepared using MQ-grade water.

All the experiments were performed at 25 °C, under argon atmosphere (1 atm), and using a VSP (Bio-Logic) potentiostat in a three-electrode cell. To avoid the dissolution and redeposition of the counter electrode material on the working electrode, the counter electrode was a carbon plate, and the reference electrode was either an aqueous mercury sulfate electrode (MSE: $Hg|Hg_2SO_4|K_2SO_4$, saturated) for acidic media or a freshly prepared reversible hydrogen electrode (RHE) for experiments in alkaline solution. A new RHE was prepared every 2 h of experiments to avoid any bias in the reference potential value; all potential values (even for acidic media) are expressed on the RHE scale.

As stated in the Introduction, this paper intends to study whether alkaline media are more aggressive (or not) than acidic ones toward state-of-the-art fuel cell electrocatalysts. The present work was performed in the frame of a larger study that is devoted to the oxidation of complex noncarbon fuels of the borohydride and nitrogen families ($NaBH_4$, NH_3BH_3, $N_2H_4BH_3$),[11−13] and it was first chosen to perform experiments

DOI: 10.1021/acscatal.5b01037
ACS Catal. 2015, 5, 4819−4824

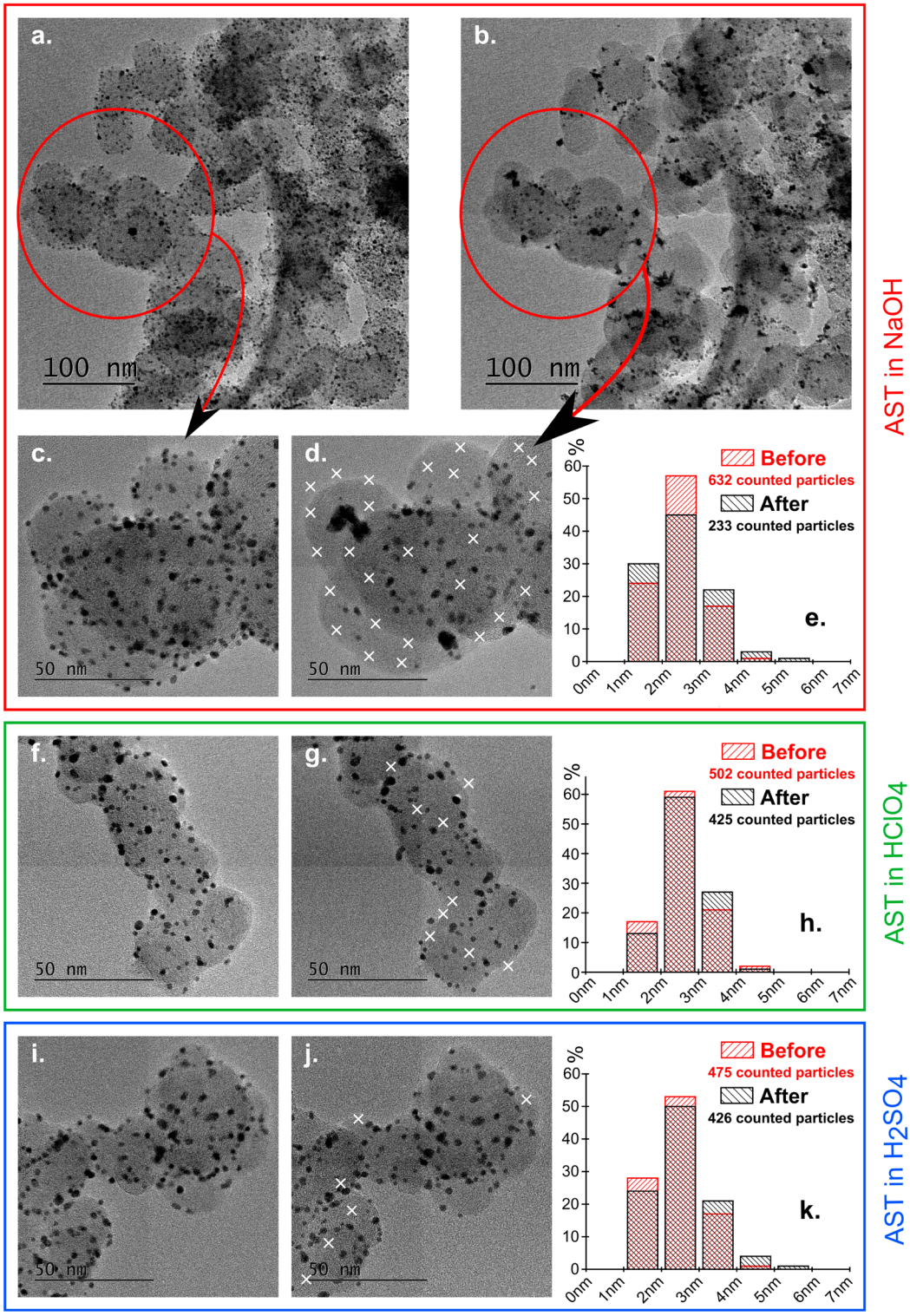

Figure 2. ILTEM micrographs pre- and post-AST at 25 °C in NaOH (a–d), $HClO_4$ (f, g) and H_2SO_4 (i, j). The white ×'s highlight the nanoparticles' loss (in a non-comprehensive manner). Corresponding nanoparticle size distribution histograms in (e) NaOH, (h) $HClO_4$, and (k) H_2SO_4. The number of particles counted on the ILTEM images before and after the AST demonstrate the much larger loss of nanoparticles in alkaline medium than in acidic ones.

in pure NaOH to verify how this solution impacts the Pt/C morphology. Therefore, the potential domain studied corresponds to that useful for the characterization of the oxidation of these fuels. As such, the AST consists of 150 cycles between 0.1 and 1.23 V vs RHE at 100 mV s^{-1} in the electrolyte solution (0.1 M H_2SO_4, $HClO_4$, or NaOH). Each AST precedes and is preceded by two measurements: (i) 15 cycles in 0.1 M H_2SO_4 (50 mV s^{-1}, between 0.1 and 1.33 V vs RHE) called a *characterization test* (Figure 1a,c,e,g) and then (ii) a *CO-stripping test* (6 min of CO adsorption; followed by 39 min of Ar purge at 0.15 V vs RHE; followed by 3 cycles in 0.1 M H_2SO_4, 20 mV s^{-1}, between 0.1 and 1.33 V vs RHE; Figure

DOI: 10.1021/acscatal.5b01037
ACS Catal. 2015, 5, 4819–4824

1b,d,f). The CO-stripping voltammograms were used to measure the ECSA of the Pt/C electrocatalysts prior to and after each AST, and the corresponding values enabled calculation of the relative ECSA losses upon each AST.

The results were then compared and correlated to the ILTEM data, in which each AST was reproduced directly on TEM grids (gold + lacey carbon), and the same regions were observed before and after the degradation test. The TEM micrographs were obtained on a JEOL 2010 TEM apparatus equipped with a LaB_6 filament operating at 200 kV (point-to-point resolution = 0.19 Å) and used to build particle-size distribution (PSD) histograms (roughly more than 400 isolated nanoparticles being counted for statistical relevance) in Figure 2e,h,k. As in ref 14, it was chosen to count the Pt nanoparticles exactly in the same regions before and after the AST, to evaluate in a quantitative manner the nanoparticles loss upon each AST.

Raman spectroscopy was used to examine the structure of the fresh and aged carbon supports. Raman spectra were recorded ex situ using a Renishaw InVia spectrometer with the near-IR line of LASER diode (785 nm). The Raman photons were collected on a Peltier-cooled CCD detector, and the spectral resolution was ~1 cm^{-1}. The measurements were performed with a ×50 LF objective, and the LASER power was ~0.2 mW on the sample. For the sake of comparison, the Raman spectra were normalized to the intensity of the peak at ~1350 cm^{-1}, which corresponds to the band of the disordered graphitic lattice-surface layer edge. For Raman spectroscopy measurements, 40 μL of catalyst ink was deposited on the glassy carbon support to avoid a support contribution, according to the procedure detailed in ref 8.

X-ray photoelectron spectroscopy was performed on a XR3E2 spectrometer (Vacuum Generator) having a Mg Kα (1253.6 eV) X-ray source powered at 300 W (15 kV, 20 mA). The kinetic energy of the photoelectrons was measured using a hemispherical electron analyzer working in the constant pass energy mode (30.0 eV). The analysis chamber was kept below 10^{-9}–10^{-10} mbar background pressure during the data acquisition, which was performed for 0.1 eV increments, at 50 ms dwelling times. The analyses were performed at an angle of 90° between the Pt/C sample surface and the analyzer. The charging effect was corrected by referring all the binding energies to the graphene component of the carbon C1s peak at 284.3 eV.[8]

3. RESULTS AND DISCUSSION

The characterization and CO-stripping tests performed before and after each AST are shown in Figure 1; the comparison of the ECSA losses is given in Figure 1g for the three different media. The results show a loss of active surface-area for both acidic and alkaline media, with an average value of 57.4, 17.3, and 22.4% of loss, respectively for the NaOH, $HClO_4$, and H_2SO_4 solutions. The degradation in alkaline medium is ~3 times worse than for acidic media, whereas only a slight difference can be observed between the results obtained in $HClO_4$ and H_2SO_4. Using $HClO_4$ and H_2SO_4 solutions enabled investigation of a possible effect of the anion-adsorption strength at the Pt sites (larger for sulfate than for perchlorate anions); the anion adsorption strength explains the potential shift of Pt oxide formation visible between parts c and e of Figure 1, as previously reported in ref 15. H_2SO_4 seems slightly more aggressive than $HClO_4$, in agreement with previous results.[16,17]

The modification of the CO-stripping voltammogram after the AST clearly gives additional information; the development of a prepeak at E = 0.7 V vs RHE upon AST in alkaline medium, associated with a shift of the main peak toward a lower potential, is attributed to the agglomeration and growth (via a platinum dissolution/redeposition mechanism, or 3D Ostwald ripening) of the Pt nanoparticles on the carbon support (Figure 1b and Figure 2a–d).[18,19] In addition, the intensity of peak 2 (in Figure 1g), corresponding to the hydrogen adsorption on edge atoms of platinum particles, has significantly decreased (relatively to peak 3) for the AST in NaOH in comparison with the results obtained for the H_2SO_4 solution; this indicates a smaller number of edge atom sites and confirms the agglomeration process.

None of these features are visible in Figure 1d and f, where the CO-stripping voltammograms before and after the AST in the acidic media are nearly unchanged. The high extent of ECSA loss in alkaline medium (60% vs ~20% in acidic media) happens only for much harsher or longer degradation protocols and at higher temperatures in acidic media.[7,20] This extreme degradation for a somewhat mild AST (25 °C, 150 cycles between 0.1 and 1.23 V vs RHE), reveals the aggressiveness of the alkaline medium toward the Pt/C nanoparticles. This parallels the recent findings of Cherevko et al.: the "transient" corrosion (i.e., that which proceeds when cycling the potential in a CV) of smooth Pt surfaces in alkaline medium starts at lower potential (by ~50–100 mV) and is about twice as harsh as that in acidic medium,[10] a recent figure that agrees with the present differences of ECSA loss measured in acidic and alkaline environments. In addition, the extent of agglomeration monitored on the CO-stripping CV is observed only in acidic media in the presence of a reducing agent such as a CO atmosphere.[20,21] ILTEM imaging was performed to shed light on the morphological changes of the Pt/C catalyst and to understand the origin of the ECSA loss differences.

Figure 2 shows the micrographs obtained before and after the AST in 0.1 M solutions of NaOH, $HClO_4$, and H_2SO_4 and the associated particle size distribution histograms.

A slight increase in the Pt nanoparticles' sizes is observed in acidic media (Figure 2f, h) as a result of the Pt dissolution/redeposition mechanism, which is expected for the high/low potential vertex used in the AST.[7,20] It corresponds to a tailing of the PSD toward large nanoparticle sizes at the expense of the smaller nanoparticle sizes, which can indicate non-negligible dissolution/redeposition (3D Ostwald ripening) processes.[4,22,23] In alkaline media, Figure 2e also indicates a slight increase in the nanoparticles' size, but in this case, the PSD histograms essentially flatten. The amount both of very small nanoparticles (between 1 and 2 nm) and of larger nanoparticles slightly increased, too. The former could result from the better contrast of the micrographs after aging in NaOH (the smaller nanoparticles are better visualized then, owing to the sharp decrease in the density of the nanoparticles over the carbon (see below)). Moreover, in alkaline medium, the non-negligible agglomeration of the Pt particles evidenced by ILTEM (Figure 2a–d), explains the shape of the CO-stripping features, with a large CO-electrooxidation prepeak at 0.7 V vs RHE (attributed to the nanoparticles agglomeration[19]).

Whatever the media, particle detachment is evidenced (white markers ease the observation in Figure 2d,g,j; understanding these markers are by no means quantitative). The absolute number of Pt nanoparticles counted on the ILTEM images before and after the "acidic" AST, however, demonstrates that

DOI: 10.1021/acscatal.5b01037
ACS Catal. 2015, 5, 4819–4824

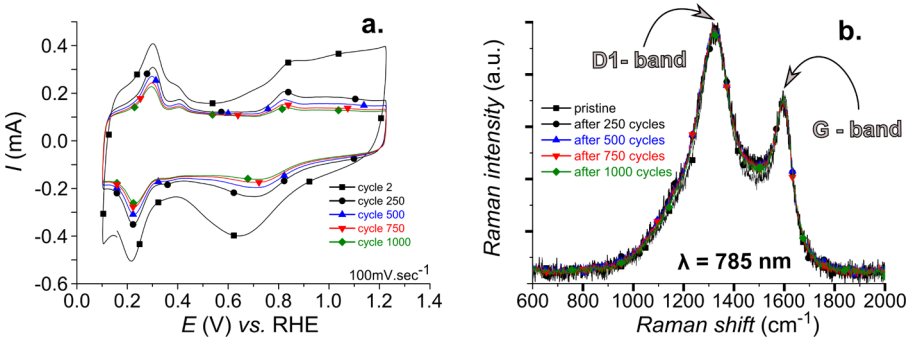

Figure 3. (a) Successive AST performed in 0.1 M NaOH at 25 °C and (b) Raman spectroscopy results (normalized) obtained after each AST.

the loss of nanoparticles after the AST (10 and 15% for an AST in H_2SO_4 and $HClO_4$, respectively) is not enough to account for all the ECSA loss (22 and 17% for an AST in H_2SO_4 and $HClO_4$, respectively). This again shows that the nanoparticle size increase (by Pt dissolution/redeposition) non-negligibly accounts for the active surface area loss electrochemically measured upon acidic AST (see Figure 1 and Figure 2f–k). On the contrary, the AST in alkaline medium yields a very large extent of Pt nanoparticle loss (63%), which matches well with the ECSA loss (57%). This shows that most of the surface area loss after the "alkaline" AST is due to the simple loss of Pt nanoparticles, not from quantitative dissolution/redeposition.

As shown in previous works, particle detachment can be linked both to a modification of the chemistry of the carbon support, which changes the interaction between the Pt particles and the support by modifying their anchoring sites on the support, and to consequent carbon corrosion in the vicinity of the nanoparticles.[7,8,23,24]

Raman spectroscopy measurements have allowed highlighting that such a huge degradation in alkaline media cannot be related to severe carbon corrosion, which is a major issue in the acidic environment of a PEMFC for long-term operation.[24] Indeed, four successive degradation tests (250 cycles in 0.1 M NaOH between 0.1 and 1.23 V vs RHE at 100 mV s^{-1} and 25 °C) have been performed, and Raman spectroscopy has been carried out on the pristine electrode and after each degradation test. Whereas Figure 3a clearly illustrates the loss of active surface area in the H_{UPD} and platinum oxides regions (the degradation being more intense during the first part of the degradation protocol, suggesting that the first cycles are the most detrimental), the Raman spectra (Figure 3b) show no special modification of the intensity of the G-band (1585 cm^{-1}, ideal graphitic lattice) and D1-band (1350 cm^{-1}, disordered graphitic lattice-graphene layer edge) vibrational modes. This indicates that no significant carbon corrosion processes happen until 1000 cycles under these conditions, which obviously rules out any carbon corrosion processes after only 150 cycles in the AST results previously reported in Figure 1 and Figure 2.

The XPS patterns of the C1s contribution (Figure 4) also show no sign of severe carbon corrosion after the AST, should it be in alkaline or acidic medium.

Finally, both the XPS and Raman data agree with the electrochemical characterizations (the double layer current hardly varies upon the AST) and the ILTEM images (no signs of severe modification of the carbon shape were observed in Figure 2a–d), thereby suggesting that the Pt nanoparticles detach from the carbon, simply following the destruction of their anchoring sites to the carbon surface. In the authors' opinion, this could follow not only the subtle modifications of

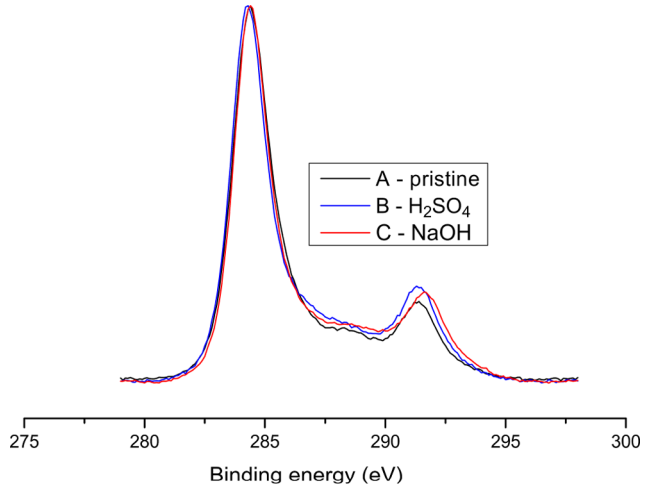

Figure 4. XPS data for the Pt/C electrocatalysts in (A) its pristine state and after the AST in (B) 0.1 M H_2SO_4 and in (C) 0.1 M NaOH.

the carbon surface chemistry in the vicinity of the platinum nanoparticle in alkaline medium, but also the harsher "transient" corrosion of the platinum surfaces in alkaline than in acidic medium,[10] which was witnessed by Cherevko et al. for larger potential values (above 1.3 V vs. RHE) than in the present work.

4. CONCLUSION

This work clearly demonstrates that an alkaline medium is really more aggressive for Pt/C catalysts than acidic ones for a given accelerated stress test (150 cycles from 0.1 to 1.23 V vs. RHE). An impressive loss of ECSA (~60%) is observed only upon AST in 0.1 M NaOH, whereas the ECSA loss is limited to ~20% in acidic media. In the latter cases, Pt dissolution/redeposition and a low extent of particle detachment have been monitored. In contrast, the huge degradation observed in alkaline medium (with respect to the extremely small number of cycles performed: 150) follows the very large loss of Pt nanoparticles (~63%). Detachment of such particles from the carbon surface is not due to extensive carbon corrosion, as demonstrated by combined ILTEM (no quantitative change of the carbon shape is detected after AST), Raman spectroscopy (no significant modification of the D1-band and G-band vibrational modes has been observed, even after 1000 cyclic voltammetry cycles), and XPS results (the C1s band is literally unchanged upon any AST). A modification of the carbon (extreme) surface chemistry in alkaline media, which modifies the anchoring sites of the particles on the support, could

DOI: 10.1021/acscatal.5b01037
ACS Catal. 2015, 5, 4819–4824

explain such degradation. More experiments will be performed to investigate this hypothesis.

AUTHOR INFORMATION

Corresponding Authors

*E-mail: Anicet.Zadick@lepmi.grenoble-inp.fr.

*Phone: +33 476826588. Fax: +33 476826777. E-mail: Marian.Chatenet@grenoble-inp.fr.

Author Contributions

¶A.Z., L.D., and M.C. contributed equally.

Notes

The authors declare no competing financial interest.

ACKNOWLEDGMENTS

The authors thank "la Region Rhône-Alpes (ARC Energies)" for funding this work. This work was performed within the framework of the Centre of Excellence of Multifunctional Architectured Materials "CEMAM" No. AN-10-LABX-44-01. Marian Chatenet thanks the French IUF for its support.

REFERENCES

(1) Vielstich, W.; Lamm, A.; Gasteiger, H. A. *Handbook of Fuel Cells*; Wiley: Chichester, 2003; Vol. *1*−*4*.

(2) Gasteiger, H. A.; Vielstich, W.; Yokokawa, H. *Handbook of Fuel Cells*; John Wiley & Sons Ltd: Chichester, 2009; Vol. *5*−*6*.

(3) Guilminot, E.; Corcella, A.; Charlot, F.; Maillard, F.; Chatenet, M. J. *J. Electrochem. Soc.* **2007**, *154*, B96−B105.

(4) Dubau, L.; Maillard, F.; Chatenet, M.; Guetaz, L.; Andre, J.; Rossinot, E. J. *J. Electrochem. Soc.* **2010**, *157*, B1887−B1895.

(5) Ferreira, P. J.; la O', G. J.; Shao-Horn, Y.; Morgan, D.; Makharia, R.; Kocha, S.; Gasteiger, H. A. J. *J. Electrochem. Soc.* **2005**, *152*, A2256−A2271.

(6) Durst, J.; Lamibrac, A.; Charlot, F.; Dillet, J.; Castanheira, L. F.; Maranzana, G.; Dubau, L.; Maillard, F.; Chatenet, M.; Lottin, O. *Appl. Catal., B* **2013**, *138*−*139*, 416−426.

(7) Nikkuni, F.; Ticianelli, E.; Dubau, L.; Chatenet, M. *Electrocatalysis* **2013**, *4*, 104−116.

(8) Castanheira, L.; Dubau, L.; Mermoux, M.; Berthomé, G.; Caqué, N.; Rossinot, E.; Chatenet, M.; Maillard, F. *ACS Catal.* **2014**, *4*, 2258−2267.

(9) Meier, J. C.; Katsounaros, I.; Galeano, C.; Bongard, H. J.; Topalov, A. A.; Kostka, A.; Karschin, A.; Schüth, F.; Mayrhofer, K. J. J. *Energy Environ. Sci.* **2012**, *5*, 9319−9330.

(10) Cherevko, S.; Zeradjanin, A. R.; Keeley, G. P.; Mayrhofer, K. J. J. J. *J. Electrochem. Soc.* **2014**, *161*, H822−H830.

(11) Olu, P.-Y.; Bonnefont, A.; Rouhet, M.; Bozdech, S.; Job, N.; Chatenet, M.; Savinova, E. *Electrochim. Acta* 2015, in press, http://dx.doi.org/10.1016/j.electacta.2015.1002.1158.

(12) Pasqualeti, A. M.; Olu, P. Y.; Chatenet, M.; Lima, F. H. B. *ACS Catal.* **2015**, *5*, 2778−2787.

(13) Belén Molina Concha, M.; Chatenet, M.; Lima, F. H. B.; Ticianelli, E. A. *Electrochim. Acta* **2013**, *89*, 607−615.

(14) Nikkuni, F. R.; Dubau, L.; Ticianelli, E. A.; Chatenet, M. *Appl. Catal., B* **2015**, *176*−*177*, 486−499.

(15) Maillard, F.; Savinova, E.; Simonov, P. A.; Zaikovskii, V. I.; Stimming, U. J. *J. Phys. Chem. B* **2004**, *108*, 17893−17904.

(16) Furuya, Y.; Mashio, T.; Ohma, A.; Tian, M.; Kaveh, F.; Beauchemin, D.; Jerkiewicz, G. *ACS Catal.* **2015**, *5*, 2605−2614.

(17) Takahashi, I.; Kocha, S. S. J. *J. Power Sources* **2010**, *195*, 6312−6322.

(18) Maillard, F.; Eikerling, M.; Cherstiouk, O. V.; Schreier, S.; Savinova, E.; Stimming, U. *Faraday Discuss.* **2004**, *125*, 357−377.

(19) Maillard, F.; Schreier, S.; Hanzlik, M.; Savinova, E. R.; Weinkauf, S.; Stimming, U. *Phys. Chem. Chem. Phys.* **2005**, *7*, 385−393.

(20) Dubau, L.; Castanheira, L.; Berthomé, G.; Maillard, F. *Electrochim. Acta* **2013**, *110*, 273−281.

(21) Zhao, Z.; Dubau, L.; Maillard, F. J. *J. Power Sources* **2012**, *217*, 449−458.

(22) Guilminot, E.; Corcella, A.; Chatenet, M.; Maillard, F.; Charlot, F.; Berthome, G.; Iojoiu, C.; Sanchez, J.-Y.; Rossinot, E.; Claude, E. J. *J. Electrochem. Soc.* **2007**, *154*, B1106−B1114.

(23) Shao-Horn, Y.; Sheng, W.; Chen, S.; Ferreira, P.; Holby, E.; Morgan, D. *Top. Catal.* **2007**, *46*, 285−305.

(24) Dubau, L.; Castanheira, L.; Maillard, F.; Chatenet, M.; Lottin, O.; Maranzana, G.; Dillet, J.; ElKaddouri, A.; Basu, S.; De Moor, G.; Flandin, L.; Caqué, N. *Int. J. Hydrogen Energy* **2014**, *39*, 21902−21914.

DOI: 10.1021/acscatal.5b01037
ACS Catal. 2015, 5, 4819−4824